

# Material optimization of carbon/epoxy composite rotor for spacecraft energy storage

**Renuganth Varatharajoo<sup>1</sup>, Mohd Sapuan Salit<sup>2</sup>,  
Goh Kian Hong<sup>1</sup>**

<sup>1</sup>Department of Aerospace Engineering

<sup>2</sup>Department of Mechanical and Manufacturing Engineering,  
University Putra Malaysia,  
43400 Selangor, Malaysia.

<sup>1</sup>E-mail: renu99@gmx.de

## ABSTRACT

An investigation to optimize the carbon/epoxy composite rotor is performed for the spacecraft energy storage application. A highspeed multi-layer rotor design is proposed and different composite materials are tested to achieve the most suitable recipe. First, the analytical rotor evaluation is performed to establish a reliable numerical rotor model. Then, finite element analysis (FEA) is employed in order to optimise the multi-layer composite rotor design. Subsequently, the modal analysis is carried out to determine the rotor natural frequencies and mode shapes for a safe operational regime below 50, 000 rpm.

**Keywords:** spacecraft flywheel, energy storage, finite element analysis

## 1. INTRODUCTION

Flywheel technology is a promising technology for replacing the conventional battery as an energy storage device for spacecraft. The flywheels can also be simultaneously used for spacecraft attitude controls [1]. One of the key elements in flywheel energy storage system is the rotor inertia, and the value of inertia is highly dependent on the rotor shape and material. The energy density is proportional to the ratio between maximum stress and density ( $\sigma/\rho$ ), which depend on the material selection. Studies have proven that the ratios between the maximum stress and the density ( $\sigma/\rho$ ) of composite materials are significantly higher than any metals [2].

Till to date, the rotor layer and material are not fully optimized. This paper provides a reasonable recipe for designing a composite rotor. It is important to point out that all the selected composite materials in this work are commercially available [3]. The stress analysis and modal analyses are engaged to investigate the flywheel rotor design. One of the notable researches on the flywheel rotor optimization is performed by Kirk et al.; however, they have only focused on the stress distribution in multi layer rotors [4]. In fact, most recent researches performed for multi layer rotors are also dedicated to stress analysis [5, 6, 7]. Instead, this current investigation is carried out for the stress distribution study incorporating the rotor dynamics (modal analysis) subjected to high rotational speeds.

Three high speed rotor configurations are investigated, i.e., single layer, double layer and triple layer rotors. The analytical and numerical stress analyses are conducted for a single layer rotor after considering the necessary properties, e.g., composite materials, rotor dimensions and rotor speeds. Then, the finite element analysis (FEA) using ANSYS<sup>TM</sup> is employed for double and triple

layer rotors' numerical stress analyses. The numerical solutions are discussed from the stress distribution point of view. In addition, the rotor dynamics are also investigated to distinguish the natural dynamic behavior of rotors during high speed operations. Finally, a suitable rotor design improvement is proposed for the space application based on the typical missions.

## 2. SPACECRAFT FLYWHEEL

The stress equations for orthotropic rotors, describing the radial displacement  $u_r$ , radial stress  $\sigma_r$  and tangential stress  $\sigma_t$  as functions of the radius are as described below [5]

$$u_r = C_1 r^k + C_2 r^{-k} - \frac{\rho \omega^2 (1 - \nu_{r\theta} \nu_{\theta r})}{9E_r - E_\theta} r^3 \quad (1)$$

$$\sigma_r = \frac{E_r(k + \nu_{\theta r})}{1 - \nu_{r\theta} \nu_{\theta r}} C_1 r^{k-1} + \frac{E_r(-k + \nu_{\theta r})}{1 - \nu_{r\theta} \nu_{\theta r}} C_2 r^{-k-1} - \frac{\rho \omega^2 (3 + \nu_{\theta r}) E_r}{9E_r - E_\theta} r \quad (2)$$

$$\sigma_\theta = \frac{E_\theta(1 + k \nu_{r\theta})}{1 - \nu_{r\theta} \nu_{\theta r}} C_1 r^{k-1} + \frac{E_\theta(1 - k \nu_{r\theta})}{1 - \nu_{r\theta} \nu_{\theta r}} C_2 r^{-k-1} - \frac{\rho \omega^2 (1 + 3 \nu_{\theta r}) E_\theta}{9E_r - E_\theta} \quad (3)$$

whereby  $k$  is a material constant,  $k = \left( \frac{E_\theta}{E_r} \right)^{0.5}$  and the Poisson's ratio for the transverse direction is  $\nu_{r\theta} = \nu_{\theta r} \frac{E_r}{E_\theta}$ . The two constants  $C_1$  and  $C_2$  can be determined after setting the rotor boundary conditions. The outer radius is a free surface where no loads are applied; thus,  $\sigma_r$  at  $r = R_o$  is null. This would be the first boundary condition for the rotor. On the other hand, the innermost rotor has to support the metallic return rings that belongs to the magnetic bearings and motor/generator magnet slots [8]. These return rings are assumed to be segmented; and therefore, no hoop stresses are permitted to exist in the material. The rings are segmented to achieve higher flywheel rotational speeds [4]. If the return rings are continuous, the performance of the flywheel would be limited since metals are vulnerable to a high stress concentration at high speeds. The segmented rings introduce pressure to the inner rotor wall during high rotational speeds, resulting radial stresses. The second boundary condition is written as:

$$\sigma_r(r = R_i) = -p_i = -\rho_{return} t_{return} R_i \omega^2 \quad (4)$$

where  $t_{return}$  is the mean return ring radial thickness and  $\rho_{return}$  is the density of return ring material (cobalt ferrite with  $\rho \approx 8150 \text{ kg/m}^3$ ). Then,  $C_2$  and  $C_1$  are estimated as given below:

$$C_2 = \frac{1 - \nu_{r\theta} \nu_{\theta r}}{\nu_{\theta r} - k} \left[ \rho \omega^2 \frac{3 + \nu_{\theta r}}{9E_r - E_\theta} R_i^k R_o^k \frac{R_i^3 R_o^k - R_i^k R_o^3}{R_o^{2k} - R_i^{2k}} + \frac{p_i}{E_r} \frac{R_o^{2k} R_i^{k+1}}{R_i^{2k} - R_o^{2k}} \right] \quad (5)$$

$$C_1 = \rho \omega^2 \frac{(1 - \nu_{r\theta} \nu_{\theta r})(3 + \nu_{\theta r})}{(9E_r - E_\theta)(\nu_{\theta r} + k)} R_o^{3-k} - \frac{\nu_{\theta r} - k}{\nu_{\theta r} + k} C_2 R_o^{-2k} \quad (6)$$

The constants depend on the rotational speed  $\omega$  of the rotor. By using Eqn. (1) and Eqn. (2), the rotor stress distributions are calculated as a function of radius for certain operating speeds. These stresses are estimated for the usable material strength. The usable

Table 1 Safety factors for IM6 Carbon/Epoxy

Parameter	Longitudinal direction	Transverse direction	
Stress	Tensile	Tensile	Compressive
Maximum strength $\sigma_{\max}$ [MPa]	3500	56	150
Vacuum fatigue coefficient	0.8	0.65	
Reciprocal safety coefficient	0.9	0.9	
Over speed factor	0.9	0.9	
Total product factor $f$	0.65	0.53	
Usable strength $f \sigma_{\max}$ [MPa]	2275	30	80

material strengths are derived from their ultimate strengths that are derated for space applications. The derated factor used for the longitudinal tensile strength is 0.65, and the derated factor of transverse tensile and compressive strength is 0.53, (see Table 1).

The reference radial thickness for the rotor analysis is based on the magnetic bearing's return rings. The return rings that are attached to the rotor have typically a mean radial thickness of less than 3 mm; thus, the minimum rotor radial thickness should be higher than this mean thickness [8]. Eqs. (1–6) can be used for a single layer rotor analytical evaluation and can serve as a reference for the numerical rotor modeling through finite element analysis (FEA). Numerical modeling is preferred for multi-layer rotors due to the complexity of their analytical solutions. Therefore, first the stress analysis is analytically and numerically carried out to establish a reasonable numerical rotor model for a single layer carbon/epoxy rotor with radii of  $R_i = 0.07$  m and  $R_o = 0.1$  m (thickness of 3 mm) and height of 0.0183 m [8]. Figures 1 and 2 show the analytical stress distributions along the transverse and tangential directions, respectively.

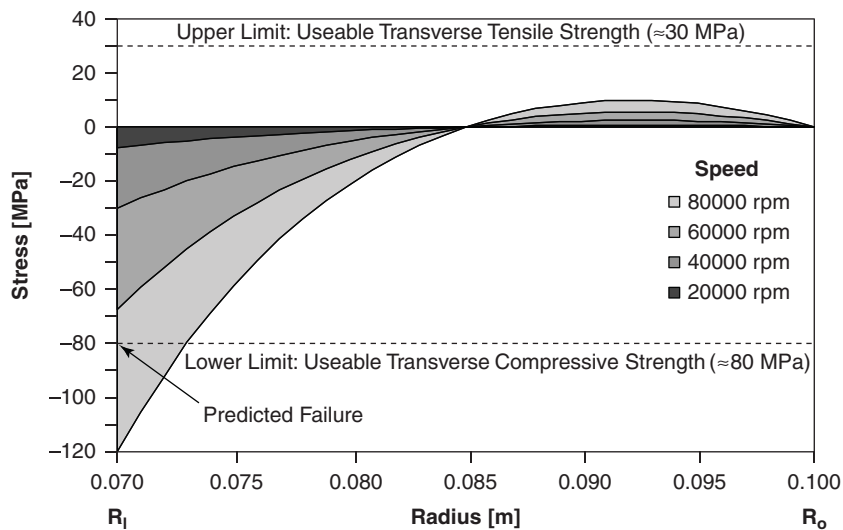


Figure 1 Transverse (radial) stress distributions.

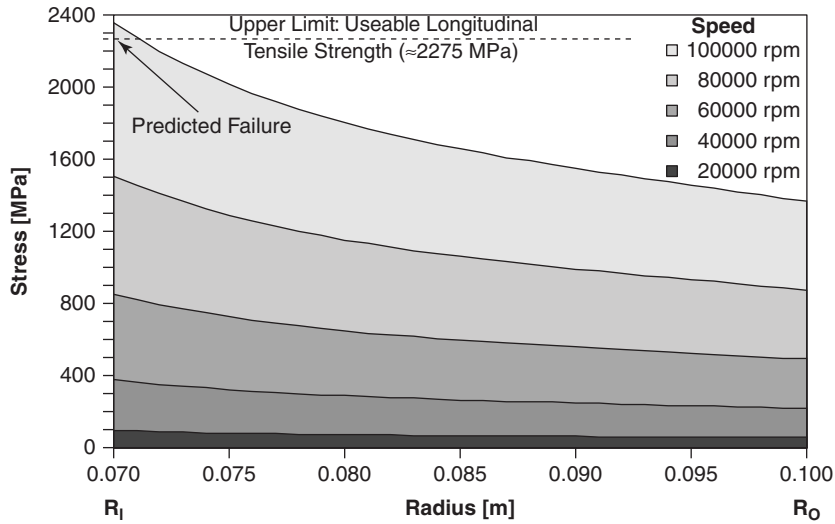


Figure 2 Tangential (longitudinal) stress distributions.

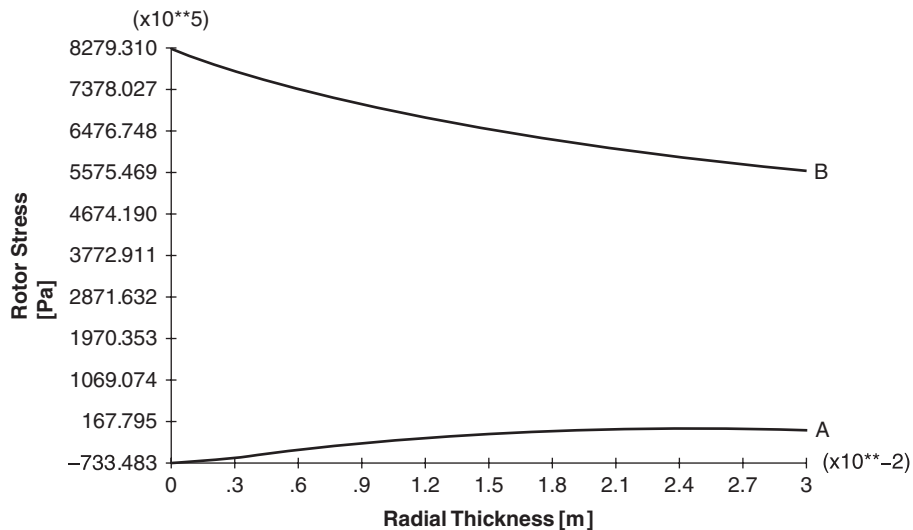


Figure 3 Transverse (A) and tangential (B) stress distributions at 60 000 rpm.

Then, a single layer rotor numerical modeling is performed using ANSYS<sup>TM</sup>. As an example, Figure 3 shows the transverse and tangential stress distributions for a rotor speed at 60,000 rpm. The numerical modeling is in agreement with the analytical solution; therefore, the numerical model can be extended to a multi-layer rotor analysis. It is important to point out that the transverse rotor compressive strength is crucial due to the return rings' pressure, and a rotor speed about 50,000 rpm seems to be the operation limit, see Figure 1. Having these two crucial criteria from the single layer rotor analysis, different carbon/epoxy composite materials are selected for the multi-layer rotors in the following section in order to determine a suitable material recipe.

### 3. CARBON/EPOXY COMPOSITE MULTI-LAYER ROTOR

#### 3.1. DOUBLE LAYER CARBON/EPOXY COMPOSITE ROTOR

The double layer 3D model is generated and analyzed by ANSYS<sup>TM</sup> with the optimized radius of  $R_i = 0.1106$  m and  $R_o = 0.1174$  m, and a rotor height  $h$  of 0.0183 m. The selected rotor dimension is suitable for small satellites (<100 kg) [8]. The operating rotational speed for the model is 50,000 rpm.

The 3D model in Figure 4 (a) displays the longitudinal/tangential rotor stress distribution MR50/LTM25 carbon/epoxy composite in the inner layer and T300/934 carbon/epoxy composite in the outer layer. A closer look at the 2D display in Figure 4 (b) shows the maximum longitudinal tensile stress of about 509 MPa appears in second layer (T300/934 carbon/epoxy composite). However, this value is well below the usable longitudinal tensile strength of this material, which is 1313.35 MPa. Having 1313 MPa of the usable longitudinal tensile strength, the inner layer also can sustain the maximum longitudinal tensile stress ( $\approx 404$  MPa). Figure 4 (c) shows the stress distribution for the transverse/radial direction. The peak transverse tensile stress of about 0.228 MPa occurs in the inner layer, and this value is lower compared to 10.865 MPa of the usable transverse tensile stress. The maximum transverse compressive strength occurs in the outer layer, which is 2.12 MPa. Besides that, 1.29 MPa maximum transverse compressive stresses occur in the inner layer. Both of the values are much lower compared to the usable transverse compressive stress that is 89.04 MPa

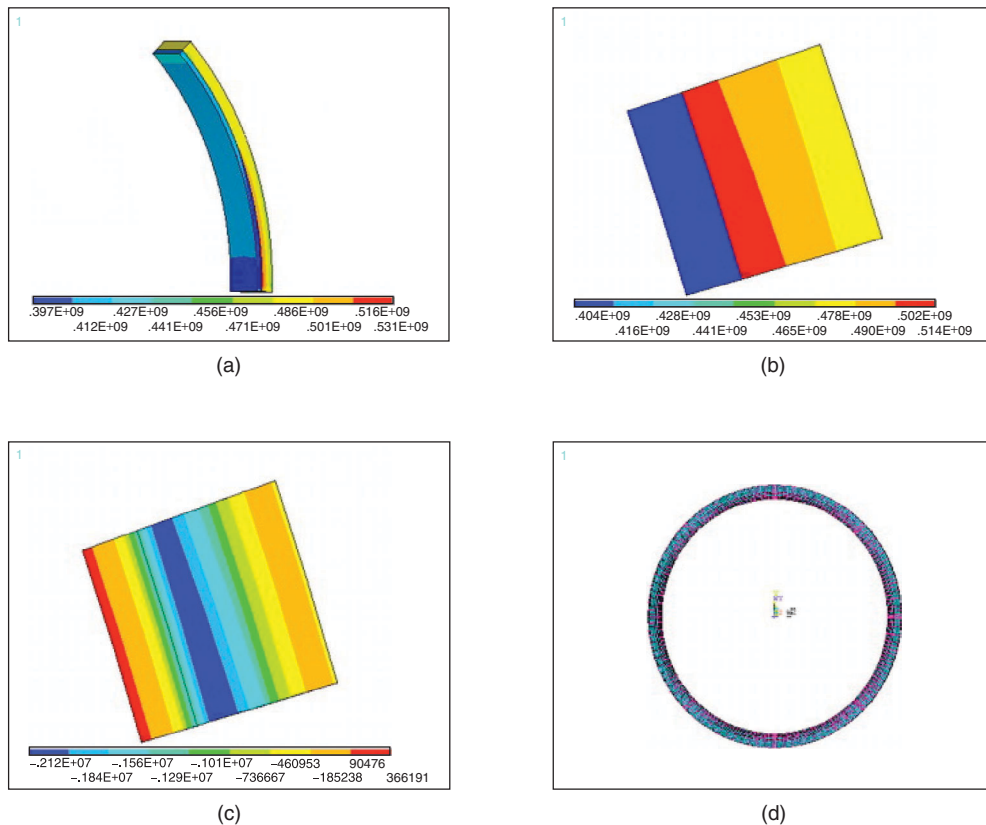


Figure 4 Double layer carbon/epoxy composite rotor.

and 76.85 MPa in the outer and inner layer, respectively. In this particular composite rotor, the maximum longitudinal tensile strength at the outer layer (509 MPa) is higher than the inner layer (404 MPa). For further enhancement, the triple layer design is proposed in order to have a better strength in the outer layer as the longitudinal tensile strength at the outer layer is obviously more critical. On the other hand, the modal analysis for this double layer rotor shows that the first natural frequency appears at 762.764 Hz or 45,766 rpm in Figure 4 (d), which is much lower than the rotor's operational frequency at 50,000 rpm. The second natural frequency is also at a lower frequency (771.667 Hz) than the operational frequency. It would be catastrophic for the missions if the natural frequency is close the operational frequency.

### 3.2. TRIPLE LAYER CARBON/EPOXY COMPOSITE ROTOR

The triple layer carbon/epoxy composite rotor with the optimized radius of  $R_i = 0.1106$  m and  $R_o = 0.1174$  m, and a rotor height  $h$  of 0.0183 m consists of AS4/3501-6 carbon/epoxy composite in the innermost layer, MR50/LTM25 carbon/epoxy composite in the middle layer and T300/934 carbon/epoxy composite in the outer layer. The operational speed of 50,000 rpm is proposed for the triple layer rotor. Figure 5 (a) shows the 3D model of triple layer carbon/epoxy composite rotor.

Figure 5 (b) shows the maximum longitudinal tensile stress occurs in the innermost layer (580 MPa) layer that is below the usable longitudinal tensile stress (1482 MPa) in this particular layer. About 386 MPa and 483 MPa longitudinal tensile stresses occur in the

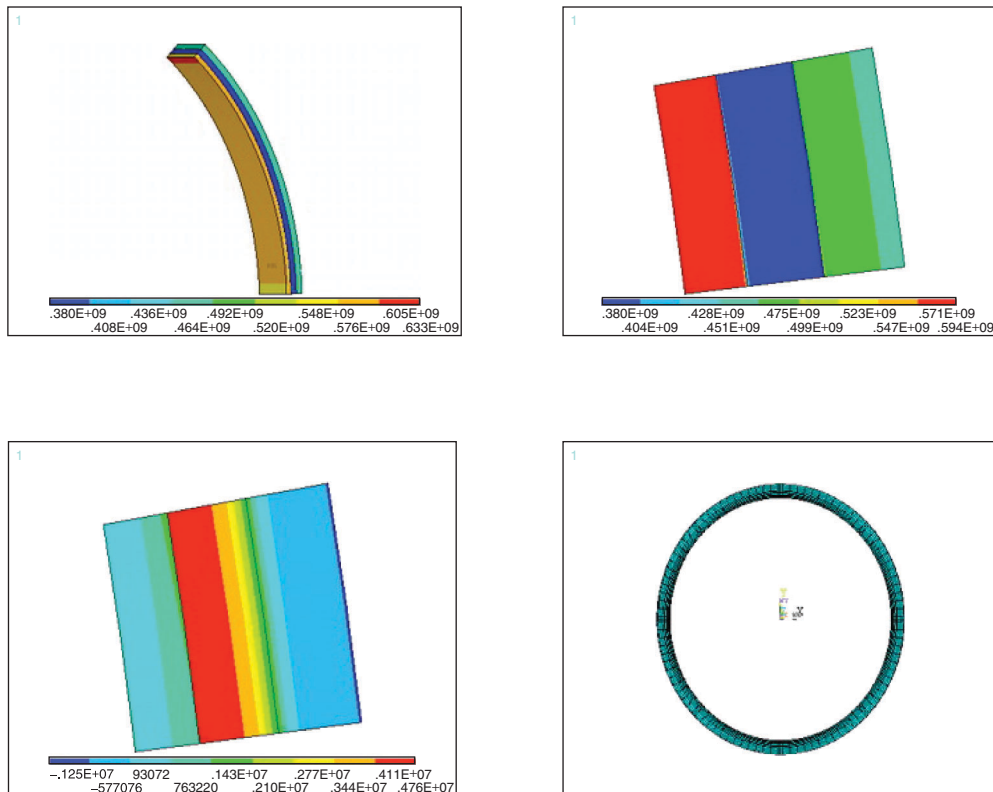


Figure 5 Triple layer carbon/epoxy composite rotor.

middle layer and outer layer in which the usable values for these layers are 1313 MPa and 1313.35 MPa, respectively. The result fulfills the condition in which the longitudinal tensile stress is more critical at the outer layer of the rotor. This combination of composites also can sustain the transverse tensile and compressive strengths as shown in Figure 5 (c). For the triple layer composite material, the modal analysis shows that the first natural frequency appears at 774.69 Hz or 46,481 rpm in Figure 5 (d), which is much lower than the rotor operation frequency at 50, 000 rpm. The second natural frequency is also at a lower frequency (788.319 Hz) than the operational frequency.

#### 4. CONCLUSIONS

From the stress distribution point of view, a thinner double layer carbon/epoxy composite rotor can be operated at a given rotor speed compared to a single layer rotor. The maximum longitudinal tensile strength at the outer layer (509 MPa) is higher than the inner layer (404 MPa) for the double layer rotor design. As the longitudinal tensile strength at the outer layer is more critical, the triple layer carbon/epoxy composite rotor would be preferred because the longitudinal tensile strength at the outer layer is lower (483 MPa). In both double and triple layer rotors, the natural frequencies limit their operations up to 50,000 rpm. The triple layer carbon/epoxy composite rotor can be operated at higher speeds up to 46,000 rpm, whereas the double layer rotor's operation is only up to 45,000 rpm. This operational speed gained in the triple layer rotor design contributes to a higher energy storage capability for the spacecraft energy storage, especially for small satellites.

#### ACKNOWLEDGEMENT

The authors would like to thank R. Kahle for the contribution of Figures 1 and 2.

#### REFERENCES

- [1] R. Varatharajoo, M. N. Filipski, Attitude performance of the spacecraft combined energy and attitude control system", *Journal of British Interplanetary Society*. vol. 57 (2004), pp. 237–241.
- [2] H. Barde, Energy storage wheel feasibility study", *Proceedings of the 4<sup>th</sup> Tribology Forum and Advances in Space Mechanisms*. No. 10, European Space Agency, Noordwijk, The Netherlands, 2001, pp. 1–26.
- [3] Composite Material Mechanical Properties, <http://composite.about.com>, 2009.
- [4] J. A. Kirk, J.R Schmidt, G. E. Sullivan, L. P. Hromada, An open core rotor design methodology, *Aerospace and Electronics Conference*. NAECON, Dayton, USA, 1997, pp. 594–600.
- [5] K. H. Sung, K. Dong-Jin, S. Tae-Hyun, Optimum design of multi-ring composite flywheel rotor using a modified generalized plane strain assumption, *International Journal of Mechanical Sciences*. vol. 43 (4) (2001), pp. 993–1007.
- [6] Y. Gawayed, F. Abel-Hady, G. T. Flowers, J. J. Trudell, Optimal design of multi-direction composite flywheel rotors, *Polymer Composites*. vol. 23 (3) (2004), pp. 433–441.
- [7] S. K. Ha, J. H. Kim, Y. H. Han, Design of a hybrid composite flywheel multi-rim rotor system using geometric scaling factors, *Journal of Composite Material*. vol. 42 (8) (2008), pp. 771–786.
- [8] R. Varatharajoo, R. Kahle, A review of conventional and synergistic systems for small satellites", *Aircraft Engineering and Aerospace Technology*. vol. 77 (2005), pp. 131–141, 2005.